PRF#: 58005-DNI6
Project Title: DNI: High-temperature Corrosion Resistance From First Principles
Principal Investigator: André Schleife, Materials Science and Engineering, U. of Illinois at Urbana-Champaign
Co-PI: none

Research progress: In the second year of this project, we focused on two topics for which it became clear that more understanding is needed, in order to ultimately obtain accurate formation energies for point defects in Al_2O_3: accurate treatment of exchange and correlation and locating the lowest-energy defect sites. First, we investigated the influence of exchange and correlation by comparing our previous results using the Perdew-Burke-Ernzerhof (PBE) generalized-gradient approximation (GGA) to two alternatives: the Strongly Constrained and Appropriately Normed (SCAN) meta-GGA and the Heyd-Scuseria-Ernzerhof (HSE06) hybrid functional. Compared to PBE, SCAN is known in the literature to offer improved accuracy at a moderately higher computational cost, while HSE06 is generally very accurate but much more computationally expensive. To assess the influence of exchange and correlation and determine the most efficient functional for our broader study of point defects and defect clusters in this system, we compared results for defect-free Al_2O_3 and Al_2O_3 with a neutral oxygen interstitial defect (O_I^x) in both the octahedral and displaced configurations across all three functionals. We found that HSE06 predicts a considerably larger Al_2O_3 band gap and O_I^x energy difference than PBE (see Table 1). Despite somewhat widening the Al_2O_3 band gap, SCAN does not improve the O_I^x energy difference over PBE. For these reasons, we conclude that PBE and SCAN are not sufficient for accurate defect formation energies in Al_2O_3 and HSE06 is necessary.

exchange-correlation functional	Al_2O_3 band gap (eV)	energy difference between O_I^x geometries (eV)	oct O_I^x – O separation (Å)	disp O_I^x – O separation (Å)
PBE	5.85	1.66	2.16	1.48
SCAN	6.71	1.58	2.16	1.48
HSE06	7.70	2.01	2.15	1.44

Table 1: Comparison of both electronic structure and atomic structure results calculated by three different exchange-correlation functionals. The band gap in defect-free Al_2O_3, the total energy difference between the octahedral (oct) and displaced (disp) O_I^x geometries, and the separation between the O_I^x defect and its nearest neighbor O atoms for both O_I^x geometries are reported.

Despite differences in electronic structure, the atomic structures calculated using PBE and HSE06 agree very well: our initial tests for V_O, O_I, Al_I, and Mg_I in various charge states and geometries revealed that atomic positions calculated with the two functionals differ by at most 0.05 Å and typically by less than 0.03 Å (see, for example, Table 1). Therefore, we can use our previously computed PBE atomic structures as starting points for HSE06 calculations, mitigating some of the additional computational expense associated with HSE06. To begin with, we have performed HSE06 calculations with reduced **k**-point sampling for several defects. In the next year, we plan to continue refining our results in this manner for more point defects and defect clusters, and we will repeat selected HSE06 calculations with a denser **k**-point grid to ensure convergence.

Additionally, we began exploring advanced approaches for locating stable interstitial sites in Al_2O_3. We have shown that for interstitial defects in this complex material, structure relaxation algorithms do not always lead directly to the lowest energy geometry; instead, depending on the initial placement of the interstitial atom, the atomic structure could relax into a configuration at a local minimum in the total energy surface. This was shown before in the literature for the oxygen interstitial, but we found that also in many other cases, the well-known octahedral site (see Fig. 1) leads to a stable configuration that does not have the lowest possible total energy. To overcome this issue, our original strategy was to displace the interstitial atom from the octahedral site before relaxation. However, after obtaining several different Al_I^x geometries depending on the direction of the initial displacement, it became clear that a more systematic approach is needed to search for the global minimum in the total energy surface.

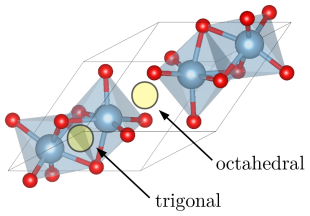

Figure 1: Schematic of the Al_2O_3 unit cell highlighting the conventional octahedral interstitial site and the newly discovered trigonal site which is energetically favorable for Al_I^x.

One idea we were pursuing uses Bayesian optimization to iteratively predict candidate interstitial sites. So far, we

applied this approach to O_I^x and Al_I^x and it not only reproduced the lowest energy structures we previously calculated, but it also found one new O_I^x geometry and eight new Al_I^x geometries. Although these new metastable geometries do not influence defect formation energies, they could have implications for defect migration paths and barriers. We are continuing to develop this method to ensure a thorough search of the available phase space.

In addition, we are testing another recently proposed approach that involves identifying high-symmetry points at Voronoi region interfaces as candidate interstitial sites [1]. Systematically testing these candidate sites produced a new, lower energy Al_I^x geometry which we previously overlooked because the interstitial site lies within a much smaller region of the unit cell, outside of the vacant octahedron containing the octahedral site (see Fig. 1). For neutral Al_I, this new geometry is 0.35 eV lower in energy than our previous minimum and 0.97 eV lower in energy than the conventional octahedral geometry. Interestingly, the lowest-energy geometry depends on the Al_I charge state (see Table 2), which could lead to diffusion mechanisms mediated by charge-transfer processes.

	Al_I^x	Al_I^{+1}	Al_I^{+2}	Al_I^{+3}
octahedral	0	0	**0**	**0**
displaced	−0.62	**−1.45**	0.25	–
trigonal	**−0.97**	−0.84	0.51	0.96

Table 2: Total energies (in eV) of interstitial aluminum defect cells taken relative to the octahedral geometry for each charge state. No stable displaced geometry has been found for an Al_I^{+3} defect. Bold indicates the lowest energy found for each charge state. Calculations were performed using the HSE06 functional with reduced **k**-point sampling.

Our new insights regarding the influence of exchange and correlation and the method developments for searching for lower energy interstitial sites enable us to compute accurate formation energies for point defects and defect clusters in Al_2O_3. They also lay the necessary groundwork for future computation of migration barriers and diffusivity in this material, since they provide the initial and final states for diffusion processes.

Career impact: The student who works 50 % on this project over the last year has made excellent progress in learning and applying cutting-edge first-principles techniques for computing defect-formation energies. This includes her exploration of different exchange-correlation functionals and also her use of the Freysoldt charge-correction scheme. Furthermore, Alina has made excellent progress in learning and exploring techniques to identify previously unknown and non-intuitive interstitial geometries. All these constitute new directions of research for the PI's group and expand our research portfolio. The PI has discussed the results outlined above with the group of Chris Van de Walle, a leading group in studies of point defects in semiconductors. This has further helped to shape the future directions of this research project. Finally, we just hired a new student who will work full time on this project over the next year, to further solidify this new direction of research in the Schleife group.

References:

[1] A. Goyal, P. Gorai, H. Peng, S. Lany, and V. Stevanović: A computational framework for automation of point defect calculations. *Computational Materials Science* **130**, pp. 1–9 (2017).